The *law of the wall*: A new perspective

Cite as: Phys. Fluids **32**, 121401 (2020); https://doi.org/10.1063/5.0036387
Submitted: 04 November 2020 • Accepted: 30 November 2020 • Published Online: 17 December 2020

Sk Zeeshan Ali and Subhasish Dey

The *law of the wall*: A new perspective

Cite as: Phys. Fluids 32, 121401 (2020); doi: 10.1063/5.0036387
Submitted: 4 November 2020 • Accepted: 30 November 2020 •
Published Online: 17 December 2020

Sk Zeeshan Ali[1,a] and Subhasish Dey[2,3,b]

AFFILIATIONS

[1] Department of Civil Engineering, Indian Institute of Technology Hyderabad, Telangana 502285, India
[2] Department of Civil Engineering, Indian Institute of Technology Kharagpur, West Bengal 721302, India
[3] Department of Hydraulic Engineering, State Key Laboratory of Hydro-Science and Engineering, Tsinghua University, Beijing 100084, China

[a] zeeshan@ce.iith.ac.in
[b] **Author to whom correspondence should be addressed:** sdey@iitkgp.ac.in

ABSTRACT

The law of the wall, regarded as one of the very few pieces of turbulence hypothesis, predicts the mean-velocity profile (MVP) in a wall-bound flow. For about nine decades, the underlying physics of the law is deemed to be governed by an *ad hoc mixing-length hypothesis*. Here, we seek the origin of the law, for the first time, with the aid of a new hypothesis, which we call the *mixing-instability hypothesis*. The hypothesis unveils the previously unknown universal scaling behavior for the amplitude of turbulent ripples or waves (that cause spontaneous stretching and shrinking of turbulent eddies) within the overlap layer and accurately maps the experimental data of the MVPs for moderate to extremely large Reynolds numbers. This study offers a new mechanism of the momentum transfer in a turbulent wall-bound flow, calling for a revision of the conventional mixing-length hypothesis, which has persisted in standard textbooks on turbulence for many decades.

I. INTRODUCTION

Turbulent flows are omnipresent in most of the natural and industrial settings. Atmospheric circulation, a swift river, flow around an airplane, and in a high-pressure pipeline are a few common examples. *The law of the wall*, coined by Coles,[1] is one of the major achievements in turbulence research. It is of great importance in a wall-bound flow because it describes the flow velocity profiles as being invariant with the streamwise length scale (i.e., self-similar velocity profiles). In fact, the law accurately predicts the flow velocity, particularly in the near-wall shear-flow layer that accounts for a considerable fraction of the aerodynamic (or hydrodynamic) drag on the wall, e.g., aircraft surfaces or pipe inner-walls.[2] Let us take the most common example of a wall-bound turbulent flow: flow in a smooth pipe or flow past a flat plate. In a steady fluid flow carrying a constant flux, the flow velocity at a given wall-normal distance z can be averaged over a sufficiently long duration to obtain the local mean-velocity u and subsequently the *mean-velocity profile* (MVP) (Fig. 1). Three separate layers exist in a wall-bound turbulent flow at an infinitely large Reynolds number, $Re \equiv UR/\nu$, where U is the bulk flow velocity (ratio of fluid flux to flow cross-sectional area), R is the length scale of the physical domain (e.g., the pipe radius or boundary layer thickness), and ν is the coefficient of the kinematic viscosity of fluid. The flow layers are conceptually sketched in the inset of Fig. 1. The first layer captures the near-wall layer (the *viscous sublayer* and *buffer layer*), being characterized by the length scale ν/u_* and the velocity scale u_*. Here, u_* is the shear velocity $[=(\tau_w/\rho)^{1/2}]$, τ_w is the wall shear stress, and ρ is the mass density of fluid. This layer roughly extends up to $z^+ = 50$, where $z^+ \equiv zu_*/\nu$. The second layer belonging beyond $z/R \approx 0.15$–0.2 characterizes a *wake layer*, where the mean-velocity is a function of u_* and the outer variable z/R. In addition, there exists an *overlap layer* between the near-wall and the wake layers. In this layer, the MVP obeys a logarithmic law as follows:[3]

$$u^+ = \frac{1}{\kappa} \ln \frac{z^+}{z_0^+}, \tag{1}$$

where $u^+ \equiv u/u_*$, κ is the von Kármán constant, z_0 is the zero-velocity level, and $z_0^+ \equiv z_0 u_*/\nu$. Following experimental observations,[4,5] we set $\kappa = 0.41$ and $z_0^+ = \exp(-5.1\kappa)$. The MVPs in a pipe flow were first obtained in 1933 by Nikuradse,[6] which have recently been adequately resolved through challenging experiments,[4,5,7–12] numerical simulations of wall-bound flow,[13–15] and the neural network model,[16] providing corridors for new research directions. However,

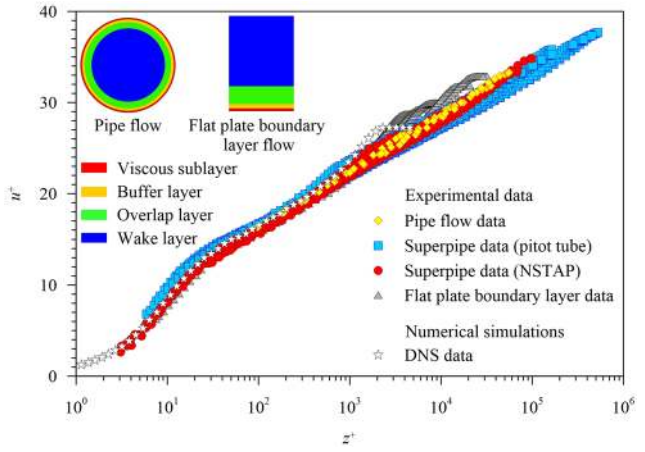

FIG. 1. MVPs on a semi-logarithmic scale, comprising data of experimental observations and numerical simulations. Each set of experimental observations (pipe flow data, superpipe data, and boundary layer data) embraces MVPs for different Reynolds numbers *Re*. The experimental observations include pipe flow data of early experiments (yellow diamonds),[6] superpipe data obtained from the pitot tube (blue squares),[4] superpipe data obtained from the nano-scale thermal anemometry probe (NSTAP) (red circles),[7,8] and flat plate boundary layer data (gray triangles);[9] numerical simulations include direct numerical simulation (DNS) data (stars).[14] The MVP ranges from the wall (defined by $z^+ = 0$) to the pipe centerline or the boundary layer thickness, which corresponds to a specific value of z^+ being dependent on *Re*. Strikingly, all MVPs in the near-wall flow layer appear to collapse on a single band. Conceptual sketches of the various flow layers in pipe and boundary layer flows are shown in the inset. Starting from the wall, as one moves along the abscissa, each MVP comprises the *viscous sublayer* (where the MVP curvature is positive), the *buffer layer* (where the MVP curvature is negative), the *overlap layer* (where the MVP curvature vanishes, obeying the logarithmic law), and the *wake layer* (where the MVP overshoots the logarithmic law).

a tangible theory appears to have lagged behind experimentations and simulations.

Equation (1) stems from the imagery of turbulent eddies that arise from strong fluid mixing in the flow.[17] Recent results have shown evidence that the turbulent eddies, being originally proposed in the derivation of the logarithmic law, correspond to the zones of coherent streamwise momentum, also called the *uniform momentum zones*.[18] The fluid mixing eventually gives rise to the turbulent shear stress. To quantify the turbulent shear stress, German aerodynamicist Ludwig Prandtl drew an analogy between the motion of turbulent eddies and that of random gas molecules. He hypothesized that a turbulent eddy preserves its entity only over a given space, called the *mixing length*, before transferring the momentum to the neighboring fluid. When the mixing length is considered to vary linearly with the wall-normal distance, the hypothesis applied to a constant stress layer (at a large Reynolds number) readily recovers the logarithmic law in Eq. (1). It is worth noting that the assumption of a constant stress layer in the derivation of the logarithmic law is debatable. Although Prandtl's idea of momentum exchange in a turbulent flow remains a cornerstone of the primitive turbulence theories, it has received criticisms for many reasons.[19–22] Among the major flaws of the mixing-length hypothesis, the first is the assumption of isotropic turbulence, wherein the root mean squares of the streamwise and the wall-normal velocity fluctuations are considered to be equal. This assumption produces an unexpected scaling of the turbulent stress in the near-wall flow layer, being incapable to meet the continuity requirement.[21] Moreover, the linear variation of the mixing length with the wall-normal distance, particularly close to the wall, is not supported by measurements.[23]

The law of the wall and its numerous analog have been predicted by means of the incomplete similarity, perturbation techniques, and intermediate asymptotics, which were extensively reviewed elsewhere,[24–26] and also via the symmetry approach.[27] In recent years, the spectral theory[28,29] and the co-spectral budget theory[30,31] have revealed a delicate link between the law of the wall and the energy spectrum of turbulent eddies (also see Ref. 32). There remains an ongoing debate as to the applicability of the logarithmic law since the MVPs for different Reynolds numbers may not strictly follow the logarithmic behavior.[33] They may however follow the power-law behavior,[34] having the Reynolds number dependent exponents with respect to a logarithmic envelope.[35,36] Despite major advances and modern refinement of the logarithmic law (see, for example, Refs. 37 and 38), Prandtl's classical work and the recent theories fall short in exploring the precise origin of the law of the wall. Here, we unveil a new mechanism that underlies the law of the wall. The new mechanism explores the missing link between the law of the wall and the mixing instability. Unlike the conventional mixing-length hypothesis, this study is not founded on the isotropic assumption. Moreover, the derivation of the logarithmic law of the wall does not necessitate any constant stress layer assumption.

II. CONCEPTUAL FRAMEWORK OF THE PROBLEM

The concept of mixing instability can be perceived from the early experiments of Osborne Reynolds, who injected a dye at the center of a pipe flow and found that the highly unstable dye streak performs a sinuous motion. Prandtl also identified that an initial wavy pattern of fluid motion led to the production of turbulence.[39] In the line of classic experiments, we envision that the turbulence manifests as the instability of fluid pathline caused by the random mixing phenomenon. The instability eventually produces turbulent ripples or waves that transmit through the fluid fabric. We consider a large Reynolds number flow so that there remains a distinct signature of the overlap layer in the flow domain. Here, we try to figure out how the turbulent shear stress is caused by the transmitting waves in a smooth pipe of radius R (Fig. 2). We denote a wetted surface W_z at a wall-normal distance z. The waves at this level are transmitted at a constant speed equaling the local mean-velocity $u(z)$. When the waves are visualized through a magnifying glass (an enlarged view shown in Fig. 2), they appear to be regular sinusoidal patterns. We focus on two successive instances, t and $t + dt$, as the waves travel through the space. At a given time t and position $x = x_1$, let the vertical line $x = x_1$ meet the waves at a characteristic point P (Fig. 2). After a short interval dt, the point P horizontally shifts to P_H, while on the line $x = x_1$, the characteristic point appears to shift vertically upward to P_V because the point of intersection of the vertical line $x = x_1$ and the waves traverses along the vertical as the time progresses. During this period, a turbulent eddy at $x = x_1$ (shown by a curved arrow in Fig. 2) experiences a wave-induced vertical motion as the waves push the eddy upward due to the vertical shift of P to

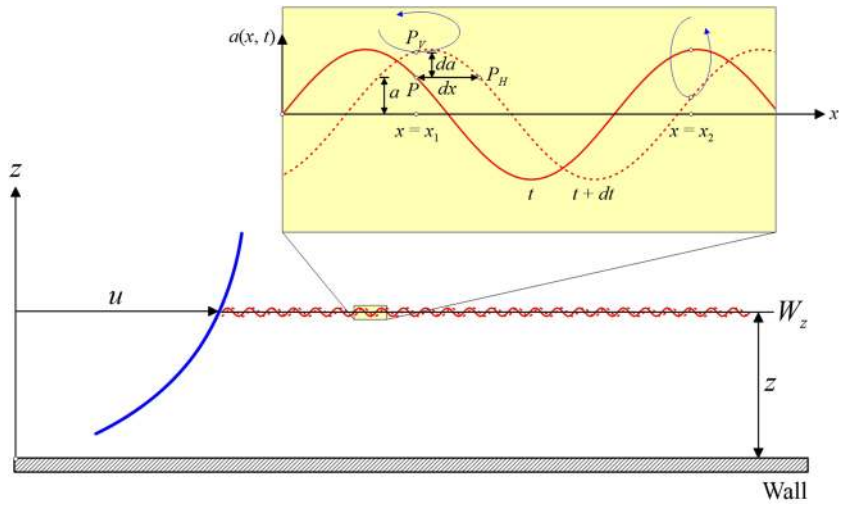

FIG. 2. Definition sketch of the mixing instability appearing as ripples or waves at an arbitrary wall-normal distance z to cause the stretching and shrinking of eddies.

P_V. Such an action causes the eddy to shrink vertically and to stretch horizontally, which is perfectly a matter of geometry. Similar stretching and shrinking of eddies prevail at any other location, say $x = x_2$ (Fig. 2), where the point of intersection of the line $x = x_2$ and the waves at time t shifts vertically downward on the line $x = x_2$ after a short interval dt. As a consequence, the waves pull the eddy downward, making the eddy to stretch vertically and shrink horizontally. Such spontaneous stretching and shrinking of eddies give rise to the turbulent shear stress.

From the above-mentioned conceptual flow physics, the *mixing-instability hypothesis* states:

> "*At a large Reynolds number, the turbulent mixing at a location in a wall-bound flow produces disturbances that transmit in the form of waves, causing continuous stretching and shrinking of turbulent eddies to produce the turbulent stress.*"

We now seek to quantify the turbulent shear stress caused by the mixing instability. When a fluid parcel carried by an eddy of characteristic volume l^3 [$\sim a^3$, $a(x, t)$ is the local amplitude of waves] is pushed upward (e.g., the eddy at the position $x = x_1$ shown in Fig. 2), the eddy is shrunk vertically by an amount $dl \sim PP_V$ ($= da$) (or $dl = cda$), where the proportionality constant c is of the order of unity. The rate of vertical shrinking is thus $(dl/dt)|_V = cda/dt$. This suggests that the eddy takes a time dt/c (slightly longer than dt) to shrink vertically by an amount da. As the eddy is also stretched horizontally (proportional to $PP_H = dx$), after a time dt/c, the rate of horizontal stretching becomes $(dl/dt)|_H = dx/(dt/c) = cu$. Therefore, the turbulent stress τ_t follows

$$\tau_t = -\rho \left.\frac{dl}{dt}\right|_V \left.\frac{dl}{dt}\right|_H = -\rho c^2 u \frac{da}{dt}. \tag{2}$$

The local amplitude $a(x, t)$ may be set as $a(x, t) = a_0 \sin(kx - \omega t)$, where a_0 is the peak amplitude, k is the wavenumber, ω is the angular frequency ($= 2\pi/T$), and T is the time period. Therefore, τ_t becomes $\tau_t = c^2 \rho a_0 u \omega \cos(kx - \omega t)$. We consider that the waves are constantly generated with a frequency $T^{-1} \sim u'$, where u' is the local velocity gradient at the wetted surface W_z, i.e., $u' \equiv du/dz$. Therefore, at any x and t, τ_t at the wetted surface W_z (i.e., at the axis of symmetry) becomes

$$\tau_t = \rho a_0 u u', \tag{3}$$

where the proportionality constant is taken as unity since its value is immaterial.

The total shear stress τ at a wall-normal distance z can be obtained from the momentum balance as $\tau = \tau_w(1 - z/R)$. τ comprises the viscous shear and the turbulent shear stresses. Therefore, we can write $\rho \nu u' + \rho a_0 u u' = \tau_w(1 - z/R)$. Introducing the friction factor $f = \tau_w/(\rho U^2)$, $a_0^+ \equiv a_0 u_*/\nu$, and the Kármán number $R^+ \equiv R u_*/\nu$, the above-mentioned equation takes the form

$$u^{+\prime} + a_0^+ u^+ u^{+\prime} = 1 - \frac{z^+}{R^+}. \tag{4}$$

For a given Re, if $z^+ \to 0$, then $a_0^+ \to 0$ (i.e., turbulent waves are unable to sustain). Equation (4) thus tends to produce $u^{+\prime} = 1$, which upon integration with the boundary condition $u^+(0) = 0$ yields $u^+ = z^+$. This is recognized as the *linear law of the wall* within the viscous sublayer.

Within the overlap layer ($z^+ \ll Ref^{1/2}$ or $z \ll R$), if we let $Re \to \infty$, then the viscous stress disappears, and Eq. (4) reduces to

$$a_0^+ u^+ u^{+\prime} = 1. \tag{5}$$

In Eq. (5), the amplitude a_0^+ of turbulent waves still remains unknown. To seek an expression for a_0^+, we consider that the waves preserve a similarity within the overlap layer. We consider a generic functional form $a_0^+ \equiv F(u^+, u^{+\prime}, u^{+\prime\prime}, u^{+\prime\prime\prime}, \ldots)$, wherein the amplitude of waves at a given wall-normal distance is dependent on the local mean-velocity and its derivatives. A first approximation considering the first even-order derivative implies $a_0^+ \equiv F(u^+, u^{+\prime}, u^{+\prime\prime})$, which upon dimensional arguments produces $a_0^+ \propto u^{+\prime}/u^{+\prime\prime}$. This

form is, however, inconsistent with the form of a_0^+ within the overlap layer [see Eq. (5)] as the dimensional analysis eliminates the term u^+. However, when the odd-order derivatives are accounted for, the function $a_0^+ \equiv F(u^+, u^{+\prime}, u^{+\prime\prime\prime})$ readily yields $a_0^+ \propto (u^{+\prime})^2/(u^+u^{+\prime\prime\prime})$, which appears to be more consistent. Moreover, the notion of odd-order derivatives is relevant here because $u^{+\prime}$ and $u^{+\prime\prime\prime}$ are linked with the shear stress and its curvature, respectively. Therefore, in order to obtain a desired scaling, we express $a_0^+ = c_s(u^{+\prime})^2/(u^+u^{+\prime\prime\prime})$, where c_s is a proportionality constant. This form of a_0^+ is indirectly evidenced by the experimental data of MVPs within the overlap layer (Fig. 1) as this unique dependency is found to recover the classical logarithmic law. When this form is substituted into Eq. (5), we obtain the following third-order ordinary differential equation:

$$u^{+\prime\prime\prime} = c_s(u^{+\prime})^3. \tag{6}$$

Equation (6) represents the governing differential equation of the MVP within the overlap layer. The solution of Eq. (6) surprisingly obeys $u^+ = c_1 \ln z^+ + c_2$ with c_1 and c_2 as constants. Setting the boundary condition $u^+(z_0^+) = 0$, the MVP follows

$$u^+ = \left(\frac{2}{c_s}\right)^{1/2} \ln \frac{z^+}{z_0^+}. \tag{7}$$

Equation (7) resembles the *classical logarithmic law* when $c_s = 2\kappa^2$ is set [compare Eqs. (1) and (7)]. With $\kappa = 0.41$, the c_s turns out to be 0.34. When this form of u^+ is substituted into Eq. (5), we obtain

$$a_0^+ = \kappa^2 \frac{z^+}{\ln\left(\frac{z^+}{z_0^+}\right)}. \tag{8}$$

The above-mentioned form can be regarded as *the universal law of turbulent waves* within the overlap layer. Note that the above-mentioned form no longer applies within the buffer and the wake layers. Within the buffer layer, the amplitude of waves is more likely to dampen due to the viscous action. An appropriate choice within the buffer layer is to consider an exponential damping by an amount of $\exp(-z^+/c_d)$, where c_d is the damping constant. Here, we set $c_d \approx 26$ to obtain a good congruence with the experimental data of the MVP. On the other hand, within the wake layer, the amplitude of waves tends to vanish as $z^+ \to Ref^{1/2}$ (or $z \to R$). Therefore, a generic expression for the amplitude of waves, in order to stretch Eq. (8) within the buffer and the wake layers, can be intuitively set as

$$\begin{aligned} a_0^+ &= \kappa^2 \frac{z^+}{\ln\left(\frac{z^+}{z_0^+}\right)} \Gamma_b \Gamma_w, \quad \Gamma_b = 1 - \exp\left(-\frac{z^+}{c_d}\right), \\ \Gamma_w &= \frac{\left[1 - z^+/(Ref^{1/2})\right]^{1/2}}{1 - c_w[z^+/(Ref^{1/2})]\left[1 - z^+/(Ref^{1/2})\right]^{1/2}}, \end{aligned} \tag{9}$$

where c_w is the wake constant being of the order of unity. Equation (9) satisfies all the plausible boundary conditions, viz., $a_0^+(z^+ \to 0) = 0$ (very close to the wall), $a_0^+(Ref^{1/2} \gg z^+ > 0) = \kappa^2[1 - \exp(-z^+/c_d)]z^+/\ln(z^+/z_0^+)$ (within the buffer layer), $a_0^+(Ref^{1/2} \gg z^+ \gg 0) = \kappa^2 z^+/\ln(z^+/z_0^+)$ (within the overlap layer), and $a_0^+(z^+ \to Ref^{1/2}) = 0$ (at the edge of the wake layer).

Equation (9) is plotted in Fig. 3. To calculate the friction factor f, we consider the following implicit equation: $1/f^{1/2} = 2.359 \ln(5.66Ref^{1/2}) - 7.679/(Ref^{1/2})^{0.55} - 1.344$.[40] This form is

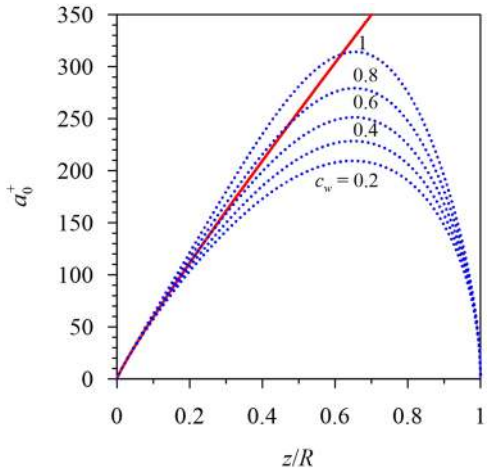

FIG. 3. Law of turbulent waves [solid line, given by Eq. (8)] and the theoretical predictions for $Re = 10^6$ and different values of c_w [dotted lines, given by Eq. (9)].

valid for moderate to extremely large Reynolds numbers so far achieved in laboratory settings. Within the overlap layer, the amplitudes of waves for different values of c_w approach the solid line, given by Eq. (8). However, within the wake layer (i.e., beyond the overlap layer), the amplitude of waves, for a given c_w, increases with an increase in z/R, attaining a peak, and afterward, it reduces with z/R. Moreover, for a given z/R, the amplitude of waves increases with an increase in c_w. Note that the peak amplitude for a given c_w appears to increase as c_w increases.

III. COMPUTATIONAL RESULTS

With Eq. (9), the MVP can be readily obtained. The edge of the viscous sublayer is set to $z^+ = 5$. It turns out that for $z^+ < 5$, the MVP obeys a linear law, given by $u^+ = z^+$, whereas beyond $z^+ = 5$, the MVP is to be determined by solving Eq. (5) subject to the boundary condition $u^+(5) = 5$. The computed results are shown in Fig. 4. For a given wake constant c_w [Fig. 4(a)], the MVPs for different Reynolds numbers Re clearly distinguish three flow layers—near-wall (the viscous sublayer and buffer layer), overlap, and wake layers. The MVPs for different Re form a logarithmic envelope. As Re increases, the extent of the overlap layer also enhances (i.e., the logarithmic law is preserved over a prolonged range of the wall-normal distance). The theoretical curves also predict the departure of the MVPs from the logarithmic law, particularly within the wake layer. However, as the wake constant c_w changes [Fig. 4(b)], the MVPs for different Re are affected only within the wake layer. For a higher value of c_w, the MVPs within the wake layer overshoot the logarithmic law, while for a lower value of c_w, the MVPs underestimate the logarithmic law.

To test the theoretical predictions of the MVPs for different Reynolds numbers Re, we collate the experimental measurements conducted in a superpipe facility.[4,7,8] The experiments were carried out using a high-pressure air facility, covering a broad range of Re. Two different instruments were used to measure the local mean-velocity, such as the pitot tube[4] and the NSTAP.[7,8] The detailed

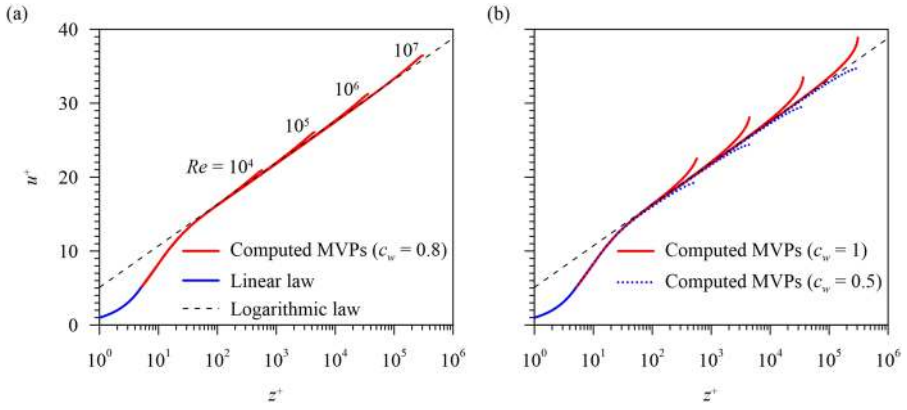

FIG. 4. (a) MVPs for different Reynolds numbers *Re* using c_w = 0.8 (red lines). The linear law (blue line) and the logarithmic law (dashed line) are also shown. (b) The same as in (a) but using c_w = 1 (solid lines) and 0.5 (dotted lines).

experimental conditions used for the validation are given in Table I. Figures 5(a) and 5(b) show the comparison of the theoretical MVPs with the experimental data. Here, the wake constant is set to c_w = 0.9, in order to obtain a good matching between the theoretical predictions and the experimental observations over a wide spectrum of the Reynolds number. the c_w = 0.9 can therefore be set as the recommended value for predicting the MVPs in a pipe flow.

TABLE I. Experimental conditions used for the validation of MVPs.

Superpipe data	U (m s^{-1})	u_* (m s^{-1})	Re	R^+
Pitot probe	3.876	0.209	1.58×10^4	8.52×10^2
	17.53	0.799	7.29×10^4	3.32×10^3
	13.11	0.558	1.55×10^5	6.6×10^3
	8.439	0.324	5.12×10^5	1.97×10^4
	19.478	0.7	1.17×10^6	4.2×10^4
	6.928	0.233	3.04×10^6	1.02×10^5
	11.504	0.366	6.8×10^6	2.16×10^5
	29.306	0.879	1.76×10^7	5.28×10^5
NSTAP	9.48	0.463	4.07×10^4	1.99×10^3
	8.4	0.369	1.23×10^5	5.4×10^3
	9.37	0.383	2.56×10^5	1.05×10^4
	10.53	0.404	5.28×10^5	2.03×10^4
	10.5	0.380	1.04×10^6	3.76×10^4
	10.57	0.348	2.98×10^6	9.81×10^4

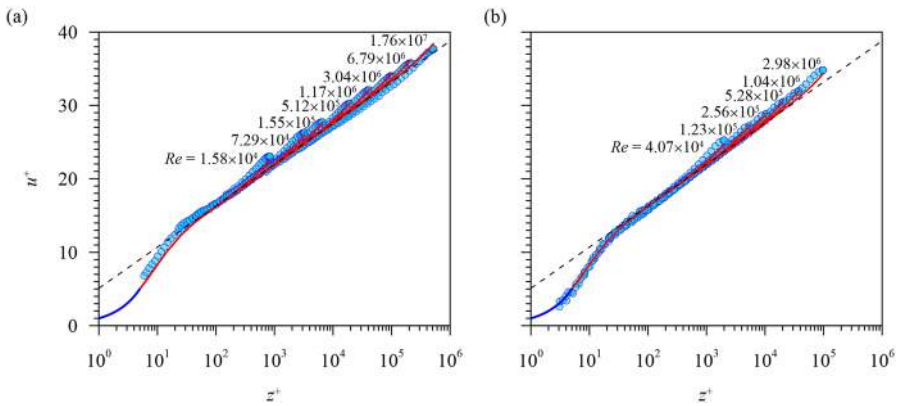

FIG. 5. Comparison of the theoretical MVPs with the experimental data obtained in a superpipe facility using (a) the pitot probe and (b) the NSTAP.

IV. CONCLUSION

We report an unprecedented link between the law of the wall and the mixing instability, hypothesizing that the turbulent mixing produces disturbances that transmit in the form of waves, causing a continuous stretching and shrinking of turbulent eddies. This mechanism sheds new light on the momentum transfer that gives rise to the turbulent shear stress. The *newly coined mixing-instability hypothesis* recovers the classical logarithmic law within the overlap layer in a completely independent way by means of a similarity consideration at infinitely large Reynolds numbers. Particularly, the amplitude of waves within the overlap layer reveals a unique scaling law with the wall-normal distance. Within the near-wall and the wake layers, the amplitude of waves encompasses damping and wake constants, respectively, which govern the damping effects within the buffer layer and the augmentation of peak amplitude prior to its attenuation toward the edge of the wake layer. More broadly, our hypothesis explains the law of the wall within the near-wall layer (characterized by the linear law within the viscous sublayer and the velocity slowdown within the buffer layer), the overlap layer (characterized by the logarithmic law), and the wake layer (characterized by the MVP overshooting the logarithmic law). Rigorous testing of the theoretical MVPs with the experimental observations over a wide range of the Reynolds number underpins the novel hypothesis.

ACKNOWLEDGMENTS

S.D. acknowledges the J. C. Bose Fellowship Award in pursuing this work. We are thankful to Alexander J. Smits for providing the experimental data.

DATA AVAILABILITY

The data that support the findings of this study are available from the corresponding author upon reasonable request.

REFERENCES

[1] D. Coles, "The law of the wake in the turbulent boundary layer," J. Fluid Mech. **1**, 191–226 (1956).
[2] I. Marusic, R. Mathis, and N. Hutchins, "Predictive model for wall-bounded turbulent flow," Science **329**, 193–196 (2010).
[3] H. Tennekes and J. L. Lumley, *A First Course in Turbulence* (MIT Press, Cambridge, MA, 1972).
[4] M. V. Zagarola and A. J. Smits, "Mean-flow scaling of turbulent pipe flow," J. Fluid Mech. **373**, 33–79 (1998).
[5] B. J. McKeon *et al.*, "Further observations on the mean velocity distribution in fully developed pipe flow," J. Fluid Mech. **501**, 135–147 (2004).
[6] J. Nikuradse, "Strömungsgesetze in rauhen rohren," Verein Deutscher Ingenieure, Forschungsheft **361**, 1–22 (1933).
[7] M. Hultmark *et al.*, "Turbulent pipe flow at extreme Reynolds numbers," Phys. Rev. Lett. **108**, 094501 (2012).
[8] M. Hultmark *et al.*, "Logarithmic scaling of turbulence in smooth- and rough-wall pipe flow," J. Fluid Mech. **728**, 376–395 (2013).
[9] S. C. C. Bailey *et al.*, "Obtaining accurate mean velocity measurements in high Reynolds number turbulent boundary layers using Pitot tubes," J. Fluid Mech. **715**, 642–670 (2013).
[10] C. M. de Silva *et al.*, "High spatial range velocity measurements in a high Reynolds number turbulent boundary layer," Phys. Fluids **26**, 025117 (2014).
[11] R. Baidya *et al.*, "Distance-from-the-wall scaling of turbulent motions in wall-bounded flows," Phys. Fluids **29**, 020712 (2017).
[12] N. Furuichi *et al.*, "Further experiments for mean velocity profile of pipe flow at high Reynolds number," Phys. Fluids **30**, 055101 (2018).
[13] S. Hoyas and J. Jiménez, "Scaling of the velocity fluctuations in turbulent channels up to $Re_\tau = 2003$," Phys. Fluids **18**, 011702 (2006).
[14] J. A. Sillero, J. Jiménez, and R. D. Moser, "One-point statistics for turbulent wall-bounded flows at Reynolds numbers up to $\delta^+ \approx 2000$," Phys. Fluids **25**, 105102 (2013).
[15] S. Tardu, "On the topology of wall turbulence in physical space," Phys. Fluids **29**, 020713 (2017).
[16] H. Wang *et al.*, "Predicting the near-wall velocity of wall turbulence using a neural network for particle image velocimetry," Phys. Fluids **32**, 115105 (2020).
[17] S. B. Pope, *Turbulent Flows* (Cambridge University Press, Cambridge, UK, 2000).
[18] M. Heisel *et al.*, "On the mixing length eddies and logarithmic mean velocity profile in wall turbulence," J. Fluid Mech. **887**, R1 (2020).
[19] M. R. Doshi and W. N. Gill, "A note on the mixing length theory of turbulent flow," AIChE J. **16**, 885–888 (1970).
[20] P. Bradshaw, "Possible origin of Prandt's mixing-length theory," Nature **249**, 135–136 (1974).
[21] F. Obermeier, "Prandtl's mixing length model—Revisited," Proc. Appl. Math. Mech. **6**, 577–578 (2006).
[22] A. J. Hutchinson, "Application of a modified Prandtl mixing length model to the turbulent far wake with a variable mainstream flow," Phys. Fluids **30**, 095102 (2018).
[23] H. Eckelmann, "The structure of the viscous sublayer and the adjacent wall region in a turbulent channel flow," J. Fluid Mech. **65**, 439–459 (1974).
[24] G. I. Barenblatt and A. J. Chorin, "New perspectives in turbulence: Scaling laws, asymptotics, and intermittency," SIAM Rev. **40**, 265–291 (1998).
[25] R. L. Panton, "Review of wall turbulence as described by composite expansions," Appl. Mech. Rev. **58**, 1–36 (2005).
[26] R. L. Panton, "Composite asymptotic expansions and scaling wall turbulence," Philos. Trans. R. Soc. A **365**, 733–754 (2007).
[27] Z.-S. She, X. Chen, and F. Hussain, "Quantifying wall turbulence via a symmetry approach: A Lie group theory," J. Fluid Mech. **827**, 322–356 (2017).
[28] G. Gioia *et al.*, "Spectral theory of the turbulent mean-velocity profile," Phys. Rev. Lett. **105**, 184501 (2010).
[29] G. Gioia and P. Chakraborty, "Spectral derivation of the classic laws of wall-bounded turbulent flows," Proc. R. Soc. A **473**, 20170354 (2017).
[30] G. G. Katul *et al.*, "Co-spectrum and mean velocity in turbulent boundary layers," Phys. Fluids **25**, 091702 (2013).
[31] G. G. Katul and C. Manes, "Cospectral budget of turbulence explains the bulk properties of smooth pipe flow," Phys. Rev. E **90**, 063008 (2014).
[32] S. Z. Ali and S. Dey, "Impact of phenomenological theory of turbulence on pragmatic approach to fluvial hydraulics," Phys. Fluids **30**, 045105 (2018).
[33] B. Cipra, "Mathematics: A new theory of turbulence causes a stir among experts," Science **272**, 951 (1996).
[34] M. Gad-El-Hak and P. R. Bandyopadhyay, "Reynolds number effects in wall-bounded turbulent flows," Appl. Mech. Rev. **47**, 307–365 (1994).
[35] G. I. Barenblatt, "Scaling laws for fully developed turbulent shear flows. Part 1. Basic hypotheses and analysis," J. Fluid Mech. **248**, 513–520 (1993).
[36] G. I. Barenblatt and A. J. Chorin, "A mathematical model for the scaling of turbulence," Proc. Natl. Acad. Sci. U. S. A. **101**, 15023–15026 (2004).
[37] F. Laadhari, "Refinement of the logarithmic law of the wall," Phys. Rev. Fluids **4**, 054605 (2019).
[38] H. Li, D. Wang, and H. Xu, "Improved law-of-the-wall model for turbulent boundary layer in engineering," AIAA J. **58**, 3308–3319 (2020).
[39] L. Prandtl, "Neuere ergebnisse der turbulenzforschung," Z. Vereines Deutscher Ingenieure **77**, 105–114 (1933).
[40] B. J. McKeon, M. V. Zagarola, and A. J. Smits, "A new friction factor relationship for fully developed pipe flow," J. Fluid Mech. **538**, 429–443 (2005).